31st Annual International Conference of the IEEE EMBS
Minneapolis, Minnesota, USA, September 2-6, 2009

The Thalamocortical Circuit and the Generation of Epileptic Spikes in Rat Models of Focal Epilepsy

Dean R. Freestone *GSMIEEE*, David B. Grayden *MIEEE*, Alan Lai, Timothy S. Nelson, Amy Halliday, Anthony N. Burkitt *SMIEEE* and Mark J. Cook

***Abstract*— We investigate thalamocortical interactions in the tetanus toxin and the cortical stimulation rat models of epilepsy. Using local field potential recordings from the cortex and the thalamus of the rat, the nonlinear regression index is calculated to create the direction index in order to study neurodynamics during seizures. Coarse time-scale analysis reveals that the cortex drives the thalamus for the majority of the time during seizures. However, fine time-scale analysis provides evidence that epileptic spikes are driven from the thalamus. This new result has implications for understanding, diagnosing and using electrical stimulation to treat epileptic seizures.**

I. Introduction

Focal epilepsy is a chronic disease of the brain affecting 60 million people worldwide [1]. The method by which epileptic seizures initiate, spread, and terminate are poorly understood. The most common feature of epileptic seizures is the spike-wave discharge. It can be observed via electroencephalography (EEG) making it the gold standard for the diagnosis of epilepsy. Recently, there have been a number of publications discussing the importance of thalamocortical (TC) interactions from both human and animal studies demonstrating that the thalamus acts as an extension of a cortical epileptic network during electrographic seizures [2]. Also mean-field mathematical models studying simulated seizures have demonstrated that the brain's dynamics may approach the epileptic state via abnormalities in the TC loop [3].

A large and perhaps critical short-coming of some previous experimental studies regarding the TC loop is the low temporal sampling of local field potential (LFP) recordings and low analysis resolution with respect to the time course of neural activity. For example, the rat TC loop has a propagation delay in the range 8-60 ms [4], [5]. If a sampling rate of 256 Hz was used the record LFPs, only 9 samples would be available to study synchrony when using a 35 ms processing window. This number of samples is insufficient to make a reliable assessment of synchrony of LFPs, indicating higher sampling rates should be used. In this study, a sampling rate of 3051 Hz was used to characterize synchrony and directionality of TC coupling.

The objective of this study was to examine the temporal sequences of activity in the TC loop on both a fine and coarse time-scale with emphasis on investigating epileptic spike generation.

II. Rat Models of Focal Epilepsy

A. Tetanus Toxin Model of Temporal Lobe Epilepsy

The well-established tetanus toxin (TT) model of epilepsy was used to produce spontaneous seizures in rats [7]. The model is implemented by a focal injection of tetanus toxin into a target region of the brain and approximately 2 to 5 days later the rat begins to exhibit spontaneous seizures. Injection of the toxin into the hippocampus results in behavioral changes that closely resemble focal seizures with secondary generalization in humans.

For our experiments, activated tetanus toxin (50 ng) was stereotaxically injected into the right hippocampus of three male inbred Sprague-Dawley rats to induce spontaneous tonic-clonic seizures, as a model of temporal lobe epilepsy.

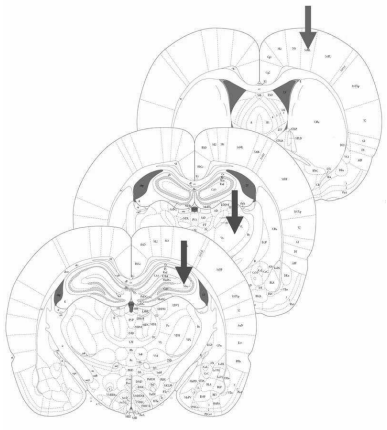

Fig. 1. Three coronal sections adapted from [8] (with permission) showing the electrode placement and tetanus toxin injection sites. The front section (-3 mm bregma) shows the tetanus toxin injection site, the middle section (-4 mm bregma) shows the thalamic electrode placement target, and the rear section shows the cortical electrode array target (0 mm bregma).

This work was supported by the Australian Research Council Linkage Grant LP0560684. The Bionic Ear Institute acknowledges the support it receives from the Victorian Government through its Operational Infrastructure Support Program

D. Freestone, D. Grayden and A. Burkitt are with the Department of Electrical and Electronic Engineering, University of Melbourne and The Bionic Ear Institute, 384 Albert St, East Melbourne, Victoria, 3002, Australia dfreestone@bionicear.org, {grayden, aburkitt} @unimelb.edu.au

A. Lai, T. Nelson and A. Halliday are with Bionic Technologies Australia, 384 Albert St, East Melbourne, Victoria, 3002, Australia {alai, tnelson, ahalliday} @bionicear.org

D. Grayden and A. Burkitt are with the Department of Electrical and Electronic Engineering, University of Melbourne, Parkville, Victoria, 3010, Australia

M. Cook is with the Department of Clinical Neurosciences, St Vincent's Hospital, Fitzroy, Victoria, 3065, Australia mark.cook@svhm.org.au

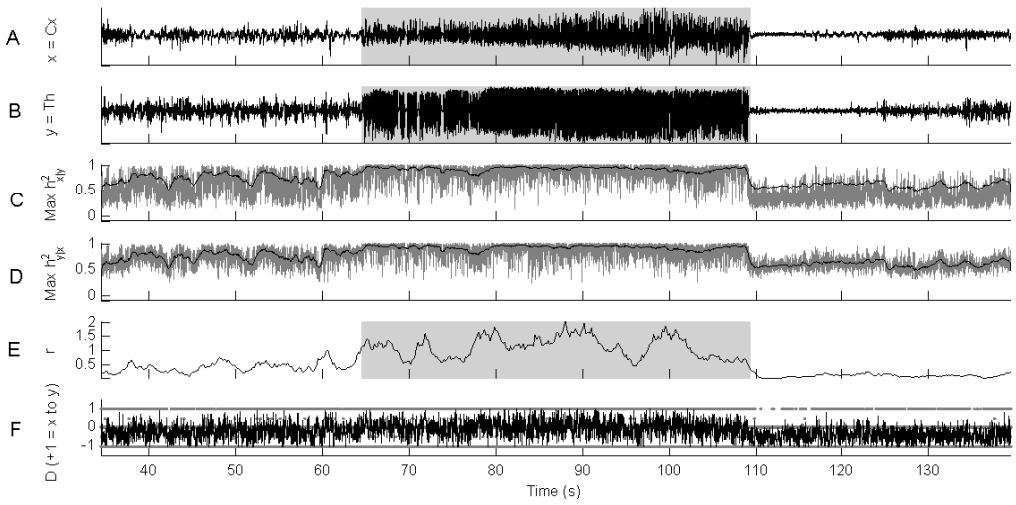

Fig. 2. Results of NLRI analysis for a seizure from a TT model rat. A) and B) show local field potential (LFP) recordings from a cortical electrode x and the thalamic electrode y respectively. C) and D) show the NLRI for the $x|y$ (or the dependance of cortex x on the thalamus y) and $y|x$ respectively. The grey traces show the raw calculation and the black traces shows a smoothed version providing a trend. E) shows the ratio of strong cortical drive to strong thalamic drive r. F) shows the direction index D (grey) and the smoothed direction index D_s (black).

Electrodes were positioned in the motor cortex and thalamus as seen in Fig. 1. Fig. 2 A and B show recordings of a seizure from a cortical and thalamic electrode respectively.

B. Cortical Stimulation Model of Focal Epilepsy

The cortical stimulation (CS) model uses high frequency (50 or 60 Hz) electrical stimulation of the motor cortex (for 1 to 2 seconds) to generate focal seizures. This method is generally accepted as a good model of focal epilepsy and has been shown to be reliable and safe [9]. Repeated cortical stimulations result in measurable epileptiform after-discharges with a high reliability of seizure initiation. The resulting seizures are similar to those seen in the amygdala kindling model in that they result in both electrophysiological and behavioral evidence of the seizure activity.

The stimulating electrodes (2x8-channel microwire array) were inserted stereotaxically into the M1 region of the motor cortex of the rat (the same position as the TT model) as seen in Fig. 1. Four interleaved pairs of the electrodes were used for recording and the remaining four were used as bipolar stimulating pairs.

III. Data Analysis

A. Nonlinear Regression Index

The nonlinear regression index (NLRI) was used to estimate the coupling strength and the direction of coupling between the cortex x and thalamus y of the rat model during seizures [6], [10]. To quantify the relationship, a curve of regression of y on x was fitted so the expected value of y given x, denoted as $\mu_{y|x}$, is calculated

$$\mu_{y|x} = \int_{-\infty}^{+\infty} y f\left(y|x\right) dy. \tag{1}$$

The NLRI measures the deviation of y from the regression curve (i.e., unexplained variance) in relation to the deviation of y from its mean (i.e., total variance), or specifically, NLRI = (total variance - unexplained variance)/total variance. If the regression curve fits the data exactly, the unexplained variance would be 0 and the NLRI equals 1. If the regression curve does not fit the data well, the unexplained variance would be large relative to the total variance and the NLRI approaches 0. The NLRI, $h^2_{y|x}$, is calculated as a function of a time delay, τ, between the discrete time signals x and y by

$$h^2_{y|x}\left(\tau\right) = \frac{\sum_{k=1}^{N}\left(y(k+\tau)-\langle y\rangle\right)^2 - \sum_{k=1}^{N}\left(y(k)-\mu_{y|x}(x(k))\right)^2}{\sum_{k=1}^{N}\left(y(k+\tau)-\langle y\rangle\right)^2} \tag{2}$$

where $\langle . \rangle$ denotes the expected value and N is the number of samples used. If the relationship between the signals is nonlinear then the dependence of y given x is different from x given y (i.e., the coupling is asymmetric: $h^2_{y|x} \neq h^2_{x|y}$). Fig. 2 C and D show examples of $h^2_{x|y}$ and $h^2_{y|x}$, respectively. The time delay, τ, can be negative or positive, corresponding to a lead or lag in the signals (with respect to each other). The delay $\tau_{y|x}$ is the time for $h^2_{y|x}(\tau)$ to reach the maximum. The delays for $\tau_{y|x}$ and $\tau_{x|y}$ are used to calculate the delay difference, $\Delta\tau$, which infers directionality in the coupling, where

$$\Delta\tau = \tau_{y|x} - \tau_{x|y} \ . \tag{3}$$

If x strongly influences y, then $\tau_{y|x}$ will be positive and $\tau_{x|y}$ will be negative, so the difference $\Delta\tau$ will be positive. Similarly, if y strongly influences x, then $\Delta\tau$ will be negative. The degree of asymmetry of the nonlinear coupling is measured by the difference

$$\Delta h^2 = h^2_{y|x}\left(\tau_{y|x}\right) - h^2_{x|y}\left(\tau_{x|y}\right) \ . \tag{4}$$

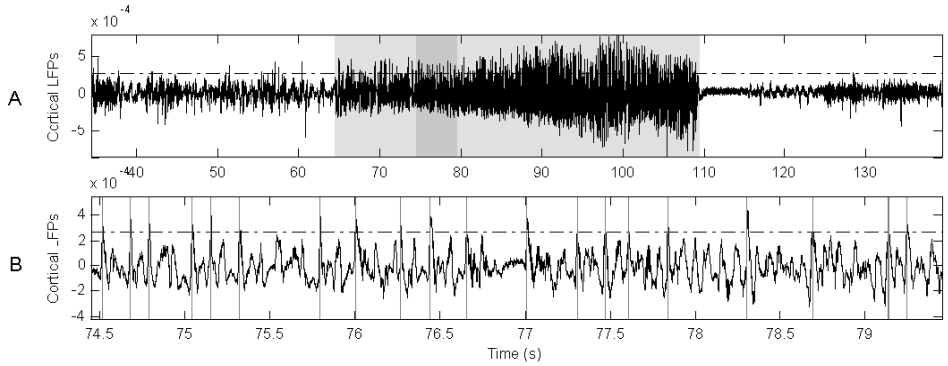

Fig. 3. Example of epileptic spike detection. A) shows the LFP recording from a seizure in a TT model rat. The light grey patch highlights the seizure. The dark grey patch highlights a time intervals that is expanded in B). The grey vertical lines mark the times where spikes have been detected. The dashed horizontal line shows in both A) and B) shows the spike detection threshold T.

If $h^2_{y|x}(\tau_{y|x})$ is larger than $h^2_{x|y}(\tau_{x|y})$, then the dependence of y on x is stronger, implying a temporal relationship (i.e., x is influencing signal y). The direction index, D, is calculated by combining Δh^2 and $\Delta\tau$ by

$$D = \frac{1}{2}\left(\mathrm{sgn}\left(\Delta h^2\right) + \mathrm{sgn}\left(\Delta\tau\right)\right) \ . \tag{5}$$

If both Δh^2 and $\Delta\tau$ are positive (or negative), then $D = +1$ (or -1), indicating a temporal relationship, $x \rightarrow y$ (or $y \rightarrow x$). If Δh^2 and $\Delta\tau$ have different signs, then $D = 0$, indicating no observed temporal relationship ($x \leftrightarrow y$). Fig. 2 F shows an example of the direction index.

In practice, $\mu_{x|y}$ is generated by a piecewise linear regression curve. The number of bins dictates how well nonlinearity can be measured (i.e., nonlinearity can be more accurately identified using more bins). Also, the number of samples per bin is important because this limits the size of the unexplained variance. Given that the EEG data was sampled at 3051 Hz, the analysis presented here used a narrow window (35 ms) allowing for sufficient samples (~ 100 using a stepped window with 90% overlap) to build the regression curve using 10 samples per bin with 10 bins.

B. Ratio of Cortical to Thalamic Drive

Using a stepped window (500 samples with 90% overlap), the number of points where $D = +1$ and $D = -1$ were summed and used to compute the ratio r where

$$r\left(n\right) = \frac{\sum_{k=m}^{k+M} D_{+1}\left(k\right)}{-\sum_{k=m}^{k+M} D_{-1}\left(k\right)} \tag{6}$$

and D_{+1}, D_{-1} is where $D(k) = 1$ and $D(k) = -1$, respectively. This ratio of strong cortical drive to strong thalamic drive provides an indication of changes in the balance of TC activity around seizures. An example is shown in Fig. 2 E. The time scale of this measure is comparable to other work in the literature [2].

C. Fine-Scale Analysis

To compare the timing of strong thalamic and strong cortical drive relative to epileptic spikes, an epileptic spike detector was implemented. Spikes were detected by comparing x to a threshold T that was 3 standard deviations, σ_x, from the mean, μ_x, of x during the seizures, which ensured that only strong, unequivocal events were detected.

$$T = \mu_x + 3\sigma_x \ . \tag{7}$$

When the amplitude of the cortical LFPs crossed the threshold, a spike was detected. To extract times of strong cortical or thalamic drive, D was smoothed using a 10th order ($M = 5$) moving average filter,

$$D_s\left(k\right) = \frac{1}{2M}\sum\nolimits_{k=m-M}^{m+M} D\left(k\right) \ . \tag{8}$$

This filter was used to prevent effects of outliers with minimal distortion on D. To detect either strong cortical drive or strong thalamic drive, D_s was compared to a threshold of 0.5 (i.e., at least 5 of 10 surrounding direction index samples must be 1 or -1). The times of the strong directionality relative to the spike detection were used to construct distributions to study the timing of thalamocortical interactions around (± 80 ms) epileptic spikes. Fig. 4 shows the timing relationships of the spikes to cortical or thalamic drive. Many low amplitude spikes and brief times of cortical or thalamic drive were ignored. This choice was made to ensure false detections did not confound the results.

IV. Results

The coarse time-scale analysis revealed an increase in cortical drive and a decrease in thalamic drive during seizures, as seen by the increase in r in the example in Fig. 2 E. This result agrees with other studies in the literature [2], [11]. The results from the fine time-scale analysis are the major contributions of this paper. Fig. 4 shows examples of strong thalamic drive preceding epileptic spikes by ~ 20 ms. This time is consistent with the expected TC propagation delay [4], [5]. The result provides evidence that the epileptic spikes are generated from thalamic drive. The distributions in Fig. 4 also show strong cortical drive on the thalamus approximately 20 ms after spikes are detected. This reinforces the notion that the 20 ms period reflects TC loop propagation delay.

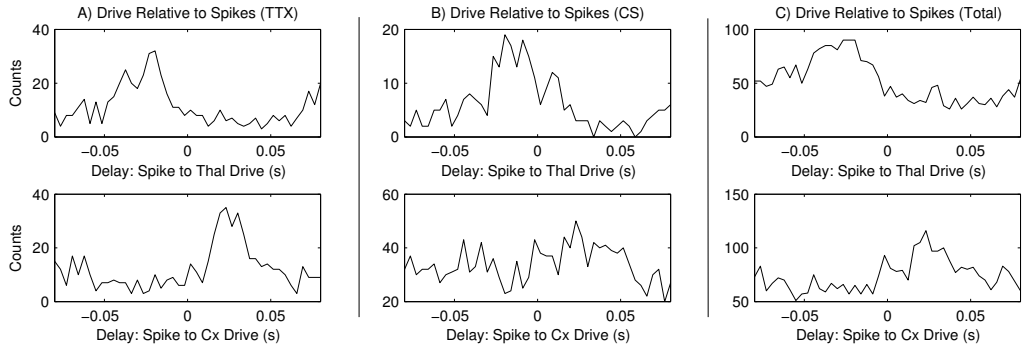

Fig. 4. Distributions relating the timing of strong drive from thalamic and cortical LFPs to the timing of epileptic spikes. The plots in the upper row relates the time of strong thalamic drive to epileptic spikes and the lower row relates strong cortical drive to epileptic spikes. Column A) shows an example from the TT model, column B) shows an example from the CS model and column C) shows the combined results from all rats.

For each of the models, the timing distributions (of thalamic and cortical drive around the spikes) were found to be significantly different ($p < 0.01$) using ANOVA testing.

V. Discussion

When considering the timing relationships from Fig. 4 some important points must be considered. Since both the cortical and thalamic signals are oscillatory, it is theoretically possible that the strong thalamic drive observed prior to the spikes may arise from the previous spike. However, this is unlikely because the delay from the cortex to the thalamus would need to be > 80 ms, which is much greater than the expected propagation delay in the TC network. Also, the observed temporal relationship could be a result of a common influence on x and y causing them to synchronize. This scenario can not be completely controlled because of finite spatial sampling with the implanted electrodes. The CS model provides the best platform to deal with possible confounding external influences on the observed signals since the seizures are generated from the stimulation electrodes that are neighboring the recording electrodes in the microarray. Therefore, in this model we know the origin of the seizures is not a confounding influence.

During the seizures, the ratio r consistently increased demonstrating that cortex influences the thalamus for more time. However, the timing distributions suggest that the cortex does not necessarily have a greater influence in sustaining the electrographic seizure. The electrographic phenomena appears to be arising from complex TC network dynamics where the spikes are generated as an epiphenomena. This has strong implications when considering that observation of spikes in electrographic seizures is the gold standard in the diagnosis of epilepsy. The fine-scale analysis reveals that causal relationships can not be assumed when using measurements that are sampled at a rate lower than what is required to capture phenomena of interest.

The distributions provide evidence that there is a self perpetuating cycle where the cortex drives thalamus which in turn drives the cortex and so on. We hypothesize that this cycle might be initiated by a brief focal cortical discharge that is not sustained over the period of the electrographic seizure. This is a promising notion when considering seizure termination via electrical stimulation. If the cycle can be broken, then the seizure may be terminated. The spike timing may be used as a stimulus timing reference, where a precisely timed electrical stimulation may interrupt the feedback loop.

VI. Conclusion

We have provided evidence that thalamic drive is crucial for the generation of epileptic spikes. This suggests that electrographic seizures initiated by focal pathologies are a large-scale network phenomena. Also, we have provided evidence that inferences of causative relationships in the brain should not be made unless sufficient temporal resolution is used.

References

[1] D. Schmidt and W. Loscher, "Drug Resistance in Epilepsy: Putative Neurobiologic and Clinical Mechanisms," Epilepsia, vol. 46, pp. 858-877, 2005.

[2] M. Guye, J. Regis, M. Tamura, F. Wendling, A.M. Gonigal, P. Chauvel, F. Bartolomei, "The role of corticothalamic coupling in human temporal lobe epilepsy," Brain, vol. 129, pp. 1917-1928, 2006.

[3] M. Breakspear, J.A. Roberts, J.R. Terry, S. Rodrigues, N. Mahant, and P.A. Robinson, "A unifying explanation of primary generalized seizures through nonlinear brain modeling and bifurcation analysis," Cerebral Cortex, vol. 16, 2006, pp. 1296-1313.

[4] Z. Tan, H. Hu, Z.J. Huang, and A. Agmon, "Robust but delayed thalamocortical activation of dendritic-targeting inhibitory interneurons," PNAS, vol. 105, 2008, pp. 2187-2192.

[5] D.L. Sherman, Y.C. Tsai, L.A. Rossell, M.A. Mirski, and N.V. Thakor, "Narrowband delay estimation for thalamocortical epileptic seizurepathways," Acoustics, Speech, and Signal Processing, 1995. ICASSP-95., 1995 International Conference on, 1995.

[6] J. P. Pijn and F. L. da Silva, "Propagation of Electrical Activity: Nonlinear Associations and Time Delays between EEG Signals," Basic Mechanisms of the EEG, 1993.

[7] J. Mellanby, C. Hawkins, H. Mellanby, J.N.P. Rawlins, and M.E. Impey, "Tetanus toxin as a tool for studying epilepsy," Journal de physiologie(Paris), vol. 79, 1984, pp. 207-215.

[8] G. Paxinos and C. Watson, The rat brain in stereotaxic coordinates, Academic Press, 2007.

[9] A. Pitkanen, P.A. Schwartzkroin, and S.L. Moshe, Models of seizures and epilepsy, Elsevier Academic Press, Amsterdam, 2006.

[10] F. Wendling, F. Bartolomei, J. J. Bellanger, and P. Chauvel, "Interpretation of interdependencies in epileptic signals using a macroscopic physiological model of the EEG," Clinical Neurophysiology, vol. 112, pp. 1201-1218, 2001.

[11] H.K.M. Meeren, J.P.M. Pijn, E. Van Luijtelaar, A.M.L. Coenen, and F.H. Lopes da Silva, "Cortical focus drives widespread corticothalamic networks during spontaneous absence seizures in rats," Journal of Neuroscience, vol. 22, 2002, p. 1480.